

# Innovative Antennas and Propagation Studies for MIMO Systems

Yoshio KARASAWA<sup>†a)</sup>, *Member*

**SUMMARY** This paper reviews our recent antennas and propagation studies for MIMO systems. First we introduce a MIMO propagation channel model in which an interesting nature can be found in eigenvalue statistics from a practical viewpoint. Then we introduce multi-keyhole model which is an efficient tool for designing a MIMO repeater systems, or MIMO radio-relay systems. For realization of compact MIMO antenna systems, effectiveness of using multiple polarizations such as dual polarizations and triple polarizations is demonstrated in multipath-rich propagation environments. With application of MIMO to OFDM systems, we focus our analysis on relation between propagation and digital transmission characteristics under a severe multipath-rich environment where the delay profile exceeds the guard interval. Finally, we discuss transmission characteristics of MIMO-OFDM with maximal ratio combining (MRC) diversity in the environment.

**key words:** MIMO, MIMO channel model, SVD, multi-keyhole, dual-polarization antenna, triple-polarization antenna, MIMO-OFDM

## 1. Introduction

In recent years, using signal processing array antennas both at the access point (or base station) and user terminals, MIMO (Multi-Input Multi-Output) has popular research field of next-generation mobile communication systems [1], [2]. The increase of system capacity without increasing the transmission power or frequency bandwidth has made the MIMO system unique and efficient in data transmission.

In Ref. [3] in 2003, we reviewed studies on MIMO propagation channel modeling. Topics highlighted in this paper are our recent study results focusing antennas and propagation-related MIMO technologies such as new channel modeling, spatial link-extension scheme, use of multiple polarizations, and frequency-domain analysis of broadband signal in frequency-selective fading environments.

In Sect. 2, we introduce a MIMO propagation channel model in which an interesting nature can be found in eigenvalue statistics from a practical viewpoint. Then we introduce a multi-keyhole model which is an efficient tool for designing MIMO repeater systems, or MIMO radio-relay systems in Sect. 3. In Sect. 4, for realization of compact MIMO antenna systems, we demonstrate the effectiveness of using multiple polarizations such as dual polarizations and triple polarizations when operating in multipath-rich propagation environments. With application of MIMO to OFDM systems, we focus our analysis on the relation be-

tween propagation and digital transmission characteristics under a severe multipath-rich environment where the delay profile exceeds the guard interval in Sect. 5. Then we discuss transmission characteristics of MIMO-OFDM with maximal ratio combining (MRC) diversity in the environment. Moreover, we introduce ongoing study topics for broadband MIMO systems with applications from wireless LAN to next-generation wireless mobile systems. Finally, we will give concluding remarks in Sect. 6.

## 2. Fundamental Properties of MIMO Channel

### 2.1 Equivalent MIMO Channel Based on SVD

MIMO channel characteristics are represented by an  $N_r \times N_t$  channel matrix ( $N_t$ : the number of transmitting antennas,  $N_r$ : the number of receiving antennas). The matrix  $\mathbf{A}$ , which is called "channel state information (CSI)" can equivalently be expressed by means of the singular value decomposition (SVD), and is given by,

$$\mathbf{A} = \mathbf{E}_r \mathbf{D} \mathbf{E}_t^H = \sum_{i=1}^{N_{\min}} \sqrt{\lambda_i} \mathbf{e}_{r,i} \mathbf{e}_{t,i}^H \quad (1)$$

where

$$\mathbf{D} \equiv \text{diag}[\sqrt{\lambda_1} \ \sqrt{\lambda_2} \ \cdots \ \sqrt{\lambda_{N_{\min}}}] \quad (2)$$

$$\mathbf{E}_t \equiv [\mathbf{e}_{t,1} \ \mathbf{e}_{t,2} \ \cdots \ \mathbf{e}_{t,N_{\min}}] \quad (3a)$$

$$\mathbf{E}_r \equiv [\mathbf{e}_{r,1} \ \mathbf{e}_{r,2} \ \cdots \ \mathbf{e}_{r,N_{\min}}] \quad (3b)$$

$$N_{\min} \equiv \min(N_t, N_r) \quad (4)$$

The vector  $\mathbf{x}^H$  denotes the complex conjugate transpose of vector  $\mathbf{x}$ ,  $\lambda_i$  is  $i$ -th eigenvalue of the correlation matrix  $\mathbf{A} \mathbf{A}^H$  or  $\mathbf{A}^H \mathbf{A}$ .  $\mathbf{e}_{t,i}$  is the eigenvector which belongs to  $\lambda_i$  derived from  $\mathbf{A}^H \mathbf{A}$ , and similarly  $\mathbf{e}_{r,i}$  is the eigenvector of  $\lambda_i$  for  $\mathbf{A} \mathbf{A}^H$ . The MIMO system possesses  $N_{\min}$  number of independent virtual channels, and each channel has a power gain of  $\lambda_i$ . Those eigenvalues of the correlation matrix vary according to the change of fading with time and frequency.

Since MIMO scheme is characterized by advanced diversity function, various diversity branches not only for multiple antennas but also for polarizations, frequency slots and so on can be utilized. As will be introduced in Sect. 4, use of dual polarizations or triple polarizations in addition to single polarization systems might be promising for realizing compact-size MIMO systems. In this case, the extended channel matrix will be used as given later (see Eq. (14)).

Manuscript received March 22, 2007.

<sup>†</sup>The author is with the Advanced Wireless Communication research Center (AWCC), The University of Electro-Communications (UEC, Tokyo), Chofu-shi, 182-8585 Japan.

a) E-mail: karasawa@ee.uec.ac.jp

DOI: 10.1093/ietcom/e90-b.9.2194

### 2.2 Statistical Distribution of Eigenvalues in i.i.d. — An Approximated Approach —

Although a number of theoretical analysis for obtaining probability density function (PDF) of eigenvalues have been carried out so far [4], [5], obtained formulae are not easy to use practically even in the case of i.i.d. (independent identically distributed) Rayleigh fading MIMO channel, particularly for larger values of  $N_t$  and  $N_r$ . For this purpose, an approximated approach based on the two interesting properties on MIMO channel statistics has been investigated [6], [7].

The properties are:

- 1) Diversity order of the  $i$ -th eigenvalue for  $N_t \times N_r$  MIMO system agrees very well with  $(N_t - i + 1)(N_r - i + 1)$ . This means that each PDF of  $\lambda_i$  follows a Gamma distribution or  $\chi$ -square distribution with freedom of  $2(N_t - i + 1)(N_r - i + 1)$ .
- 2) The ratio between averaged value of the  $i$ -th eigenvalue and the  $(i + 1)$ -th eigenvalue for  $N_t \times N_r$  MIMO and the ratio between averaged value of the  $(i - 1)$ -th eigenvalue and the  $i$ -th eigenvalue for  $(N_t - 1) \times (N_r - 1)$  MIMO have nearly the same value, namely,  $\frac{\langle \lambda_i^{(N_t, N_r)} \rangle}{\langle \lambda_{i+1}^{(N_t, N_r)} \rangle}$  is approximately equal to  $\frac{\langle \lambda_{i-1}^{(N_t-1, N_r-1)} \rangle}{\langle \lambda_i^{(N_t-1, N_r-1)} \rangle}$ .

Considering that 3) the total sum of the eigenvalues for  $N_t \times N_r$  MIMO is  $N_t N_r$  and 4) an accurate calculation formula for the averaged value of the largest eigenvalue is available [8], the PDFs for individual eigenvalues can be calculated as follows [6].

$$f(\lambda_i, v_i, \beta_i) = \frac{1}{\Gamma(v_i)} \beta_i^{v_i} \lambda_i^{v_i-1} \exp(-\beta_i \lambda_i) \quad (5)$$

where

$$v_i = (N_t - i + 1)(N_r - i + 1) \quad (6)$$

$$\beta = v_i / \Lambda_i^{(N_t, N_r)} \quad (7)$$

with

$$\begin{aligned} \Lambda_i^{(N_t, N_r)} &\equiv \langle \lambda_i^{(N_t, N_r)} \rangle \\ &\approx \frac{N_t N_r - \Lambda_1^{(N_t, N_r)}}{(N_t - 1)(N_r - 1)} \Lambda_{i-1}^{(N_t-1, N_r-1)} \end{aligned} \quad (8)$$

$$\Lambda_1^{(N_t, N_r)} \approx N_t N_r \left( \frac{N_t + N_r}{N_t N_r + 1} \right)^{2/3} \quad (N_t N_r \leq 250) \quad (9a)$$

$$\approx (\sqrt{N_t} + \sqrt{N_r})^2 \quad (N_t N_r \geq 250) \quad (9b)$$

where  $\Gamma$  is the gamma function. Results of computer simulation identified that all eigenvalues for MIMO with  $N_t \leq 5$  and  $N_r \leq 5$  calculated by the above equations give sufficient accuracy for practical use. The properties mentioned above are shown in Fig. 1 where the nature stated above is clearly seen in Fig. 1(b). Figure 2 shows cumulative distribution function (CDF) of eigenvalues of  $8 \times 4$  MIMO in

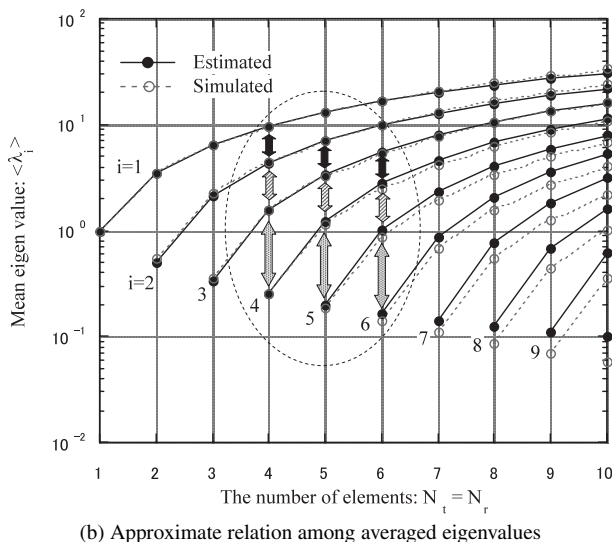
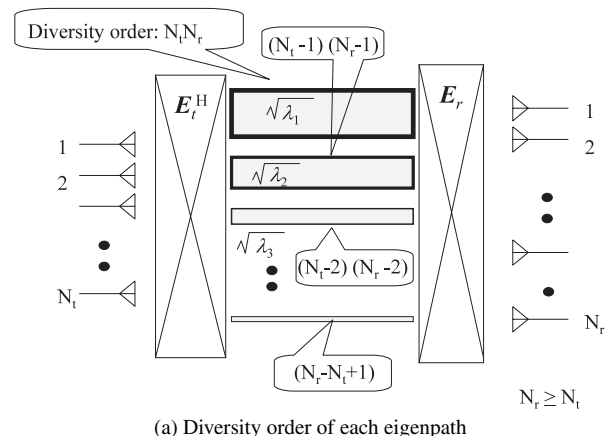


**Fig. 1** Features of MIMO channel statistics for i.i.d. Rayleigh fading environment.

i.i.d. Rayleigh fading environment. The bold solid lines show simulation results which can represent theoretical values and dotted lines give the calculation results based on the above equations. Although the shape of each curve agrees very well, a slight offset in the averaged value particularly for the smallest eigenvalue curve can be seen (order of 1 dB at most). This means that approximation by means of gamma distribution (Eq. (5)) gives sufficient accuracy in wide range of  $N_t$  and  $N_r$  values while the averaged value calculated based on Eq. (8) gives small errors when estimating the smaller eigenvalues with the larger value of  $N_t$  or  $N_r$ . By shifting the calculated curves, depicted by the thin solid lines, so as to coincide with their averaged values, we can identify the good coincidence between the two.

### 2.3 Open Questions for Non-i.i.d. Case

The above discussion ignores spatial correlation between antenna branches. In the case of base station side where the angular spread in the direction of each user terminal is relatively small, the spatial correlation must be taken into consideration. Figure 11 of Ref. [3] shows averaged eigen-

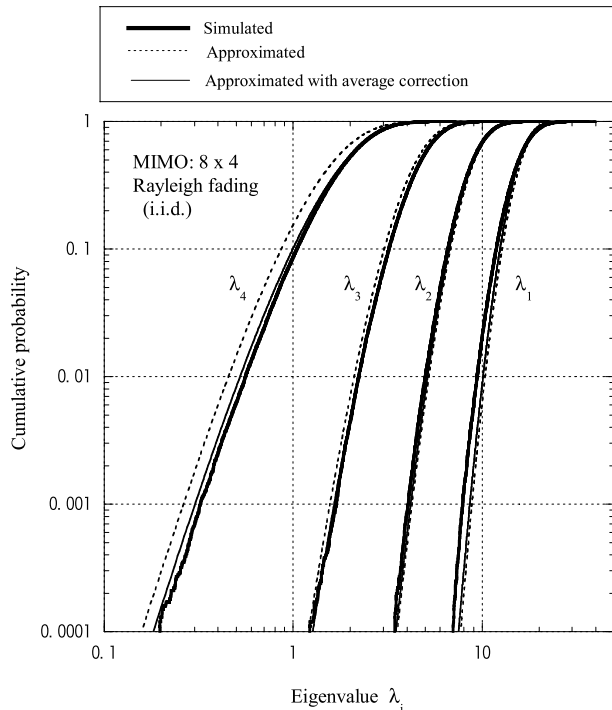


**Fig. 2** CDF of eigenvalues for  $8 \times 4$  MIMO in i.i.d. Rayleigh fading environment: Simulated vs approximated.

values obtained by simulation for  $N_t = N_r$  in the correlated case. In this case, one of the both sides only considers spatial correlation by  $\rho = 0.9$  (correlation between adjacent branches, for detail, see Ref. [3]). A common nature said in Sect. 2.2 (or Fig. 1(b)) is still effective even in the case of correlated multipath environment, that is “the ratio between the averaged value of the  $i$ -th eigenvalue and the  $(i + 1)$ -th eigenvalue for  $N_t \times N_r$  MIMO and the ratio between the averaged value of the  $(i - 1)$ -th eigenvalue and the  $i$ -th eigenvalue for  $(N_t - 1) \times (N_r - 1)$  MIMO have nearly the same value.”

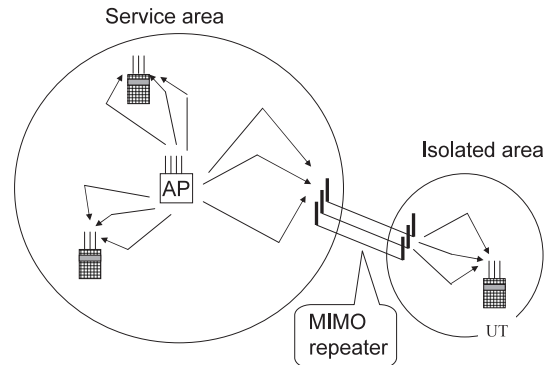
#### Open questions:

1) Utilizing the above nature, how to calculate the averaged eigenvalues simply as a function of propagation parameters such as correlation coefficients of  $\rho_t$  at a transmitting side and  $\rho_r$  at a receiving side as well as the number of antennas ( $N_t$  and  $N_r$ )?

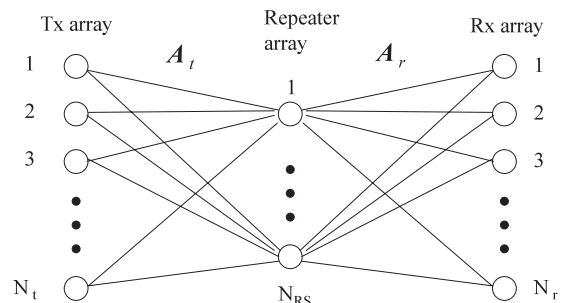
2) Does the probability distribution of each eigenvalue ( $\lambda_i$ ) follow the Gamma distribution very well? If yes, how to calculate the diversity order ( $v_i$  in Eq. (6)) in the correlated case?

### 3. Multi-Keyhole Model

As expected, MIMO can realize a high capacity system in multipath-rich environment. In order to extend such a high capacity service to an isolated area, MIMO repeater system will be promising [9] as shown in Fig. 3(a). If we extend the service to an isolated area by using a conventional repeater, only single-stream transmission can be achievable even if environments around the access point



(a) An image of MIMO repeater system



(b) A channel model (Multi-keyhole model)

**Fig. 3** MIMO repeater system and its channel model.

(AP) and a user terminal (UT) are fully multipath-rich because the number of non-zero eigenvalues comes down to one. The channel is equivalent to so-called “keyhole channel” [10]. If we adopt multiple-repeater-antenna system, multi-stream transmission, which is one of the MIMO advantage, can be achieved depending on the number of repeater antennas. From a propagation viewpoint, the channel connected through MIMO repeater is equivalent to multi-keyhole channel shown in Fig. 3(b).

The received signal vector  $\mathbf{r}$  is given by

$$\mathbf{r} = \mathbf{A}_r \mathbf{G} (\mathbf{A}_t \mathbf{s} + \mathbf{n}_{RS}) + \mathbf{n}_r \quad (10)$$

where  $\mathbf{s}$  denotes the transmit signal vector,  $\mathbf{n}_{RS}$  denotes the noise vector at the repeater system,  $\mathbf{n}_r$  denotes the noise vector at UT,  $\mathbf{A}_t$  denotes the channel matrix from AP to repeater Rx antennas,  $\mathbf{A}_r$  denotes the channel matrix from the repeater Tx antennas to UT, and  $\mathbf{G}$  denotes the gain matrix in amplitude of repeater antennas.

Assuming that the effect of the thermal noise at the repeater site is negligibly small, and that the gain  $\mathbf{G}$  is normalized by the number of the repeater antennas  $N_{RS}$ , the overall channel response matrix  $\mathbf{A}_e$  is given by

$$\mathbf{A}_e = \frac{1}{\sqrt{N_{RS}}} \mathbf{A}_r \mathbf{A}_t \quad (11)$$

Since each repeater antenna acts as a keyhole effect, we call this model “multi-keyhole model.” Although we know the PDF of amplitude of each element in the matrix  $\mathbf{A}_e$  as double-Rayleigh distribution, it seems not easy to obtain a general formula to calculate the PDF of the individual

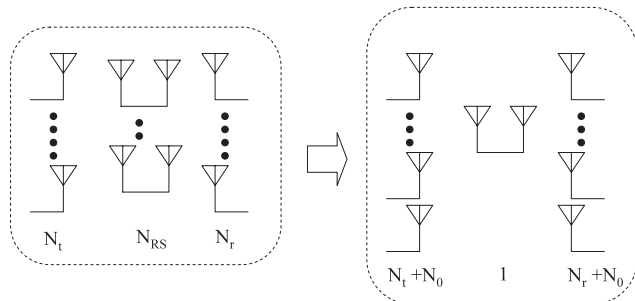


**Fig. 4** Equivalent configuration for diversity order analysis concerning the largest eigenvalue.

eigenvalues. In the case of  $N_{RS} = 1$ , which corresponds to the conventional single-keyhole environment, on the other hand, the PDF of the largest eigenvalue can be calculated by the following equation [9], [11].

$$f(\lambda_1) = \frac{2\lambda_1^{(N_t+N_r)/2-1}}{\Gamma(N_t)\Gamma(N_r)} K_{|N_t-N_r|}(2\sqrt{\lambda_1}) \quad (12)$$

where  $K_\alpha$  is the  $\alpha$ -th modified Bessel function of the second kind.

In Ref. [12], by introducing the equivalent antenna increasing number  $N_0$ , and connecting the concept said in Sect. 2.2 to the above equation, the PDF of the largest eigenvalue can be calculated by the following formula in good agreement with the simulated values.

$$f(\lambda_1) = \frac{2\lambda_1^{(N_t+N_r)/2+N_0-1}}{\Gamma(N_t+N_0)\Gamma(N_r+N_0)} K_{|N_t-N_r|}(2\sqrt{\lambda_1}) \quad (13)$$

The parameter  $N_0$ , which is not integer, is given as a function of  $N_t, N_r$ , and  $N_{RS}$  from an empirical approach (for detail, see Ref. [12]). Although the model is still under development, for the largest eigenvalue statistics, an interesting nature such that the diversity order of multi-keyhole channel  $[(N_t - N_{RS} - N_r)]$  seems equivalent to that of  $[(N_t + N_0) - 1 - (N_r + N_0)]$  (i.e. equivalent to a single-keyhole MIMO), can be seen from the equation structure, and is shown in Fig. 4. In Ref. [12], PDFs of all eigenvalues including  $\lambda_1$  have already formulated with a similar form of Eq. (13), and good coincidence between simulated and calculated has been confirmed.

#### 4. Multiple Polarizations

For practical use of MIMO systems without decreasing its channel capacity, the antenna portion is needed to be more compact. One way to do so is by utilizing the advantage of polarization diversity. Use of dual polarizations (such as horizontal polarization and vertical polarization) antenna in MIMO system has been proposed and successfully demonstrated so far [13]–[15]. In order to realize the higher channel capacity, a MIMO system having three polarization diversity branches, denoted as triple-polarization MIMO, has also been proposed in [16], [17]. In this section, we present basic configuration and characteristics of MIMO systems with multi-polarization antennas.

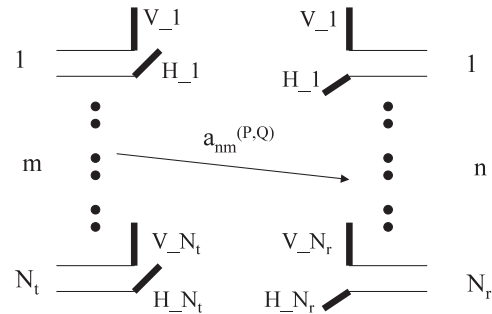


**Fig. 5** MIMO transmission systems using dual-polarization antenna arrays.

#### 4.1 Dual-Polarization Antenna System

Figure 5 shows a dual-polarization MIMO of  $2N_t \times 2N_r$  ( $= 4N_tN_r$  in total) branches consisting with  $N_t$  transmitting antennas and  $N_r$  receiving antennas. As shown in the figure, let the dual polarizations consist of vertical polarization (V) and horizontal polarization (H). The channel state information (CSI) is expressed by the channel matrix  $\mathbf{A}$  given by

$$\mathbf{A} \equiv \begin{bmatrix} \mathbf{A}^{(VV)} & \mathbf{A}^{(VH)} \\ \mathbf{A}^{(HV)} & \mathbf{A}^{(HH)} \end{bmatrix} \quad (14)$$

$$\mathbf{A}^{(QP)} \equiv [a_1^{(QP)} \ a_2^{(QP)} \ \dots \ a_m^{(QP)} \ a_{N_t}^{(QP)}] \quad (15)$$

$$\mathbf{a}_m^{(QP)} \equiv [a_{1m}^{(QP)} \ a_{2m}^{(QP)} \ \dots \ a_{nm}^{(QP)} \ a_{N_r m}^{(QP)}]^T \quad (16)$$

where, P and Q represent one of the two polarizations individually (namely, (QP) expresses one of (VV), (VH), (HV) and (HH)), and  $a_{nm}$  is the complex amplitude connecting Tx antenna of  $m$  to Rx antenna of  $n$ .

Main difference between a conventional single polarization system with i.i.d. Rayleigh fading environment and dual-polarization system with the same number of branches is mainly due to cross-polarization discrimination (XPD) between orthogonal polarization branches. The XPD is defined, for example, by

$$\mathbf{XPD} \equiv \frac{\langle |a_{nm}^{(VV)}|^2 \rangle}{\langle |a_{nm}^{(VH)}|^2 \rangle} \quad (17)$$

From a number of measurements so far, the value of XPD ranges from 0 dB to 10 dB depending on indoor and outdoor multipath environments, and a value around 5 dB is a typical value.

Figure 6 shows the average channel capacity characteristics for both single- and dual-polarization systems having  $4 \times 4$  branches as a function of  $K$  factor in the case of Nakagami-Rice fading environment which covers from LOS (line-of-sight with  $K > 1$ ) to non-LOS (Rayleigh fading with  $K = 0$ ) widely. The results were obtained through computer simulations assuming that XPD for multipath component excluding the directwave component is 5 dB. (Note that the same figure but XPD = 0 dB is given in Fig. 13 of Ref. [15], for more detail in simulation condition, see the

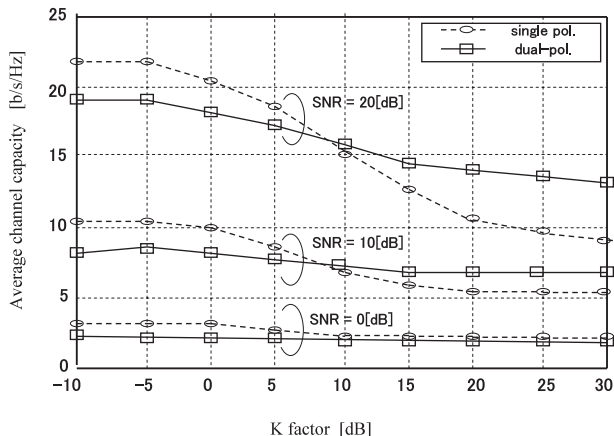


**Fig. 6** Channel capacity characteristics for both single-and dual-polarization antenna systems having 4×4 branches as a function of  $K$  factor in Nakagami-Rice fading environment.

reference.) Because of assuming XPD of 5 dB, for multipath condition near Rayleigh fading (namely  $K < 1$ , or  $< 0$  dB), the channel capacity for dual-polarization systems for the higher SNR cases shows a slightly smaller value compared with single-polarization systems. However, for larger  $K$  factor case, higher channel capacity can be achieved in dual-polarization systems. This means that dual-polarization systems can always realize two-stream transmission even in the case of LOS conditions. By utilizing this nature, two-stream transmission system applying Alamouti-type STBC scheme has been proposed in Fig. 3 of Ref. [15].

#### 4.2 Triple-Polarization Antenna System

In order to realize higher channel capacity, a MIMO system having three polarization diversity branches, denoted as triple-polarization MIMO, has been proposed in [16], [17].

Figure 7 shows the basic configuration of triple-polarization antenna. Two orthogonal polarization ports such as vertical polarization (V) and horizontal polarization (H) has been created on the same patch metal plate. And the third one (Z) has been added perpendicularly just in the middle on the circular patch. The port Z has been added in the patch antenna as though it jointly use the ground plane but does not contact with the circular patch. Thus port Z will act as an independent monopole antenna on the ground plane. By designing three orthogonal ports in this way, the polarization plane of each waveform will cross each other perpendicularly. And in a multipath-rich environment, all the three orthogonal polarization ports are expected to work as three independent antennas.

We developed this antenna for the frequency of ranging from 4.9 GHz to 5.3 GHz, so that the diameter of the ground plane is about 4 cm [17]. Antenna gains for V, H and Z are 5.6 dBi, 5.6 dBi and 2.2 dBi, respectively. Isolation between V port and H port is less than -29 dB and that between V and Z is less than -23 dB in the frequency range.

We have measured the MIMO performance in a hand-

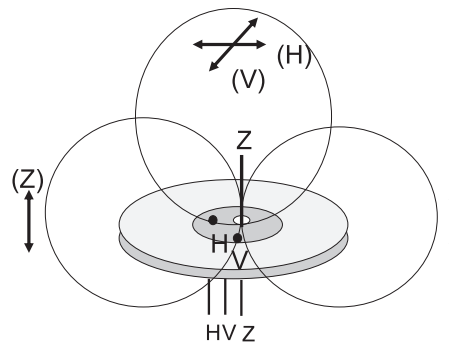


**Fig. 7** A compact MIMO antenna utilizing tri-polarizations.

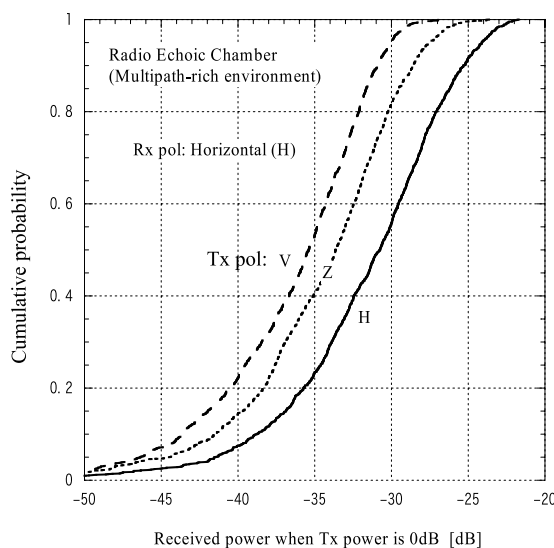


**Fig. 8** CDF of received power for H-H, V-H, and Z-H ( $f = 5$  GHz)

made radio echoic chamber where an ideal multipath-rich Rayleigh fading environment can be realized. The delay profile shows a typical exponential-decay function with the delay spread of 400 ns. All measurements were carried out using a 4-port vector network analyzer (VNA) in the frequency domain.

Figure 8 shows CDFs of received power for Tx\_pol-Rx\_pol of H-H (co-pol.), V-H (cross-pol.), and Z-H (cross-pol.) [17]. From the figure, average XPD is about 5 dB for V-H, and 3 dB for Z-H. The channel matrix  $A$  were measured as a function of frequency using the VNA. The eigenvalues of the correlation matrix  $AA^H$  were obtained as a function of frequency. Figure 9 shows the average channel capacity when using the tri-polarization antenna at both ends [17]. In the figure, marks: A, B, and C mean the cases of single-pol. (V-V:  $1 \times 1$ ), dual-pol. (V,H-V,H:  $2 \times 2$ ), and tri-pol. (V,H,Z-V,H,Z:  $3 \times 3$ ), respectively, and mark D means three-dipole array by three-dipole array (V,V,V-V,V,V:  $3 \times 3$ ) as a reference. In this figure, effectiveness of the tri-pol. antenna, the performance of which is close to the conventional  $3 \times 3$  MIMO antenna, can be identified.

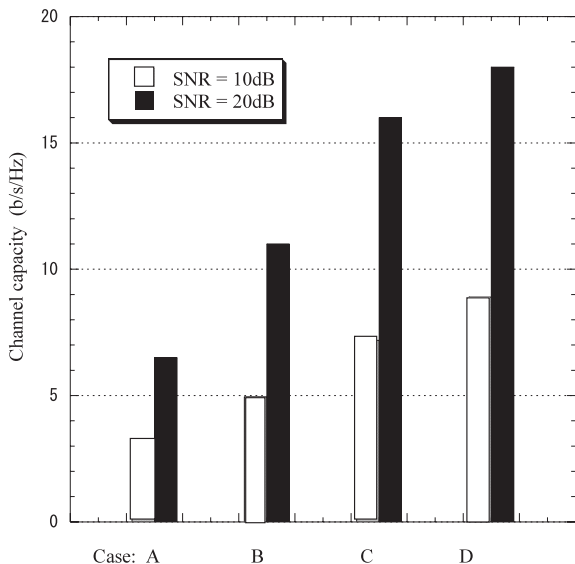


**Fig. 9** Average channel capacity when using multiple polarizations: A: single-pol. (V-V: 1 × 1), B: dual-pol. (V,H-V,H: 2 × 2), C: tri-pol. (V,H,Z-V,H,Z: 3 × 3) and D: three single-pol. antennas by three single-pol. antennas (V,V,V-V,V,V,V: 3 × 3).

## 5. Broadband MIMO Systems

### 5.1 Propagation Factors for OFDM

The Orthogonal Frequency Division Multiplex (OFDM) digital transmission scheme is a much anticipated technology among those considered for application in terrestrial digital broadcasting, wireless LAN, and next-generation mobile communication systems because OFDM is resistant to large multipath delay spread. OFDM transmits broadband signals by dividing the signals into a large number of narrowband channels to achieve resistance to such a long delay spread. In addition, a guard interval (GI) longer than the maximum delay is inserted between adjacent OFDM symbols, and a scheme called cyclic prefix (CP) is incorporated into the GI in order to completely eliminate both intersymbol interference (ISI) and concurrently occurring intercarrier interference (ICI).

Even so, a number of cases having large delay spread beyond that expected have also been reported in indoor environments surrounded by walls of metallic materials and in mobile communications. In future systems, with increasing carrier frequency and vehicular speed for outdoor operation, two different propagation factors, namely, large delay spread beyond the guard interval and large Doppler spread will cause difficulty for selecting appropriate OFDM parameter values in the system designing [18]. Figure 10 shows the necessary conditions among two propagation factors and OFDM parameters. The condition is given by,

$$\sigma_{\tau} \ll T_{GI} \ll T_s \ll T_f \quad (18)$$

└ ISI ┘
└ Efficiency ┘
└ ICI ┘

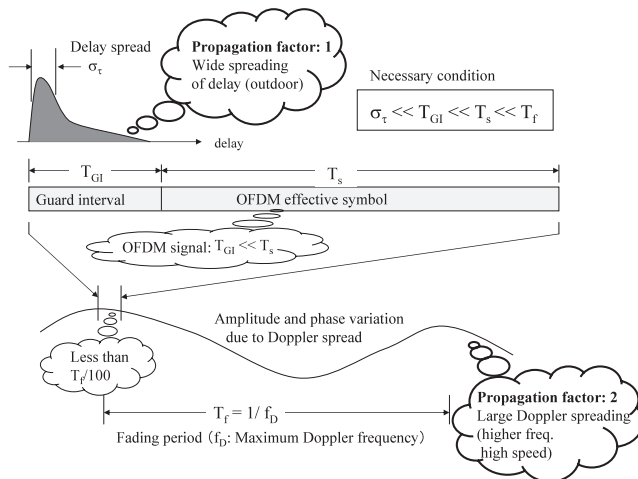


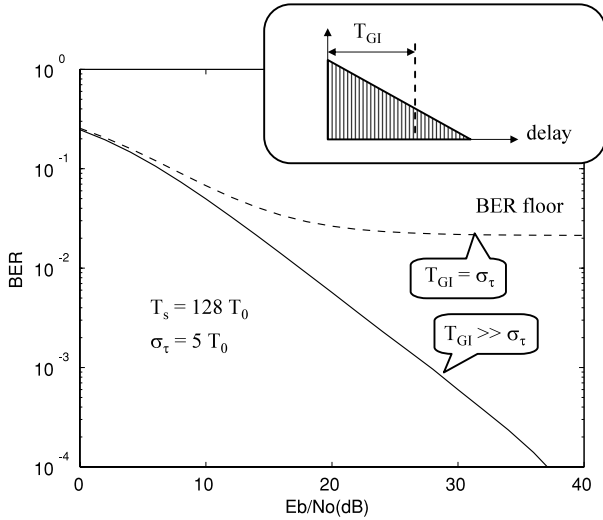
**Fig. 10** The necessary conditions among two propagation factors and OFDM parameters.

where  $\sigma_{\tau}$  is delay spread,  $T_{GI}$  is guard interval,  $T_s$  is effective OFDM symbol period, and  $T_f$  is a fading period defined by  $1/f_D$  ( $f_D$ : the maximum Doppler frequency). Assuming an outdoor operation where the delay spread is  $2\mu s$ ,  $T_{GI}$  must be larger than  $10\mu s$ . On the other hand, when the frequency is 5 GHz and vehicular speed of 30 m/s (or 108 km/h),  $T_f$  will be 2 ms which requests  $T_s$  shorter than  $20\mu s$ . Due to these incompatible demands, it seems difficult to keep high efficiency for next-generation mobile cellular systems.

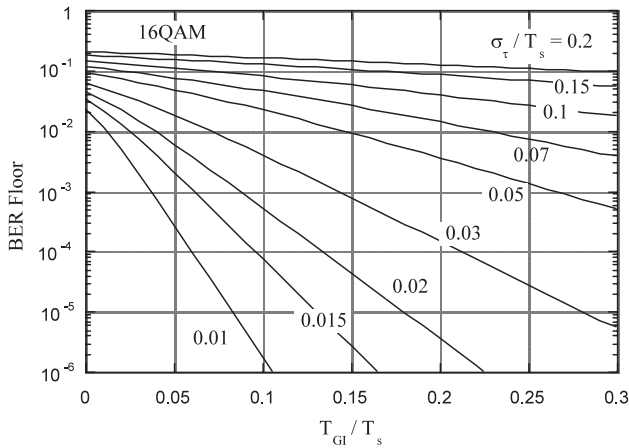
The propagation channel model for OFDM where delay profile exceeds the guard interval has been developed in Ref. [19] where we call the model “ETP (Equivalent Transmission-Path) -OFDM model.” Error floor characteristics are shown in Fig. 11. In Fig. 11(a), the floor value of BER due to ISI (with ICI) will be significant when delay profile exceeds the guard interval. Statistical OFDM transmission characteristics in terms of the BER floor for 16 QAM, which is calculated by using the ETP-OFDM model, is given in Fig. 11 (b) as a function of the propagation and system parameters.

### 5.2 MIMO-OFDM

MIMO, on the other hand, can overcome this difficulty by means of diversity function. Figure 12(a)–(d) is examples of the received power characteristics (Power: solid lines) and the error distribution statistics (BER: bar graph) for the link connecting each transmitting antenna and each receiving antenna (corresponding to four single-input single-output (SISO) cases) in  $2 \times 2$  MIMO, in fading where the delay profile exceeds the guard interval [20]. Since the thermal noise is not included in the simulation, the generated errors are due to ISI and ICI. It is clear from Fig. 12 (a)–(d) that the occurrence of these errors is concentrated at the sub-channels in which the received power is low. This is attributed to the fact that the frequency characteristics vary greatly in these regions, enhancing the waveform distortion.



(a) Occurrence of error floor



(b) OFDM transmission characteristics as a function of propagation and system parameters

**Fig. 11** BER floor characteristics of OFDM/DQPSK system when the maximum delay exceeds the guard interval.

Maximal ratio combining (MRC) is a well-established combining scheme in which the received power is maximized (i.e., the SNR under constant noise power is maximized). It is expected that the errors due to ISI will be reduced significantly by applying this scheme. In Fig. 12(e), the received power changes less, owing to the diversity effects in the MIMO configuration. The transmission error is also reduced. Thus the MIMO configuration is promising, since it is more robust to ISI than the SISO configuration. The floor value of BER for MIMO with OFDM/DQPSK after MRC is shown in Fig. 13 [20]. As is evident from the figure, when the ratio  $T_{GI}/\sigma_\tau$  is increased, the BER is decreased drastically, indicating that the condition given in Eq. (12) seems to be reduced in the case of MIMO.

Since the MIMO-OFDM introduced here is MRC diversity, the scheme is classified into a single-stream transmission. Multi-stream transmission such as eigenmode transmission robust to such a large-delay multipath environment is left as a future study.

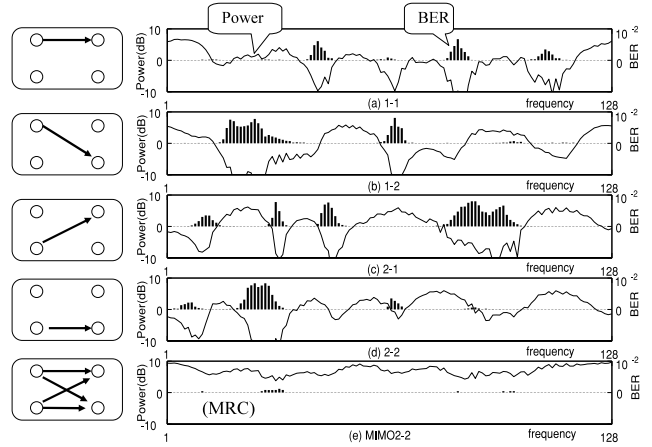


**Fig. 12** Diversity effect of 2 × 2 MIMO system.

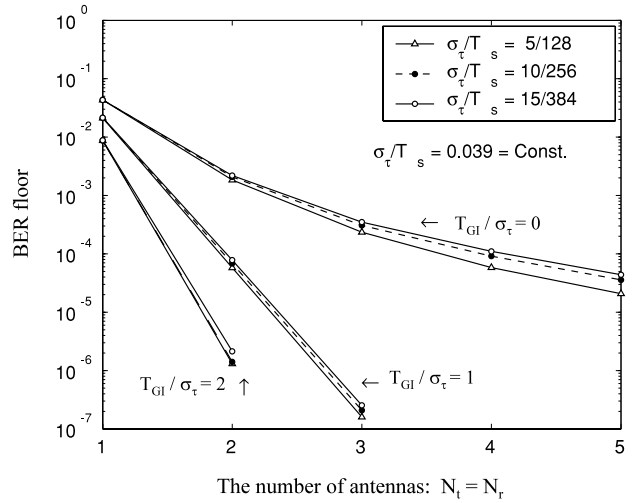


**Fig. 13** BER floor characteristics of MIMO MRC for OFDM/DQPSK.

### 5.3 MIMO for Broadband Systems

Approaches other than multi-carrier transmission schemes for wideband systems under frequency-selective fading environment are mainly classified into two categories. One is single carrier transmission with frequency domain signal processing, and the other is that with time domain signal processing. Since there are enormous studies about these technologies, we will limit to introducing our studies very briefly.

For adaptive array operation, we have confirmed that single-carrier transmission with cyclic prefix, and frequency-domain block signal processing, which is called subband signal processing, is a promising way [21]–[23]. Based on this background, subband adaptive array for space-time block coding (STBC) in single carrier MIMO transmission with cyclic prefix has been proposed [24]. A drastic computational cost reduction can be achieved without sacrificing noticeable transmission performance degradation compared with time-domain symbol-by-symbol signal pro-

cessing scheme.

For single-carrier transmission with time domain signal processing for broadband MIMO systems, narrowband signal processing scheme with spatial filtering only [25] and wideband signal processing schemes using tapped delay lines (TDLs) [26]–[28] have been proposed and analyzed. In order to overcome computational complexity, further studies must be needed in time-domain signal processing.

## 6. Conclusion

This paper dealt with antennas and propagation-related MIMO technologies. Topics highlighted in this paper are recent study results on the area carried out in our group. We deeply convinced that understanding of eigenvalue characteristics of channel matrix is the most important matter because they give all necessary information when estimating BER or channel capacity. We therefore dealt with this statistics first. Then we introduced multi-keyhole model which is an efficient tool for designing a MIMO repeater system, or MIMO ad hoc network. For realization of compact MIMO antenna systems, effectiveness of using multiple polarizations such as dual orthogonal polarizations and triple polarizations was demonstrated in multipath-rich propagation environments. With application of MIMO to wideband systems, we focused our analysis on relation between propagation and digital transmission characteristics under severe multipath delay environments. Then, the transmission characteristics of MIMO-OFDM with maximal ratio combining (MRC) diversity in the environment were discussed.

As stated, since MIMO performance depends largely on propagation environment, understanding of propagation statistics and channel model is truly essential. It is hoped that this paper will provide some valuable suggestions for future research and development in MIMO technologies.

## Acknowledgement

This work was supported in part by the Grants-in-Aid for Scientific Research (No. 17360177) from Japan Society for the Promotion of Science (JSPS) and partly from Strategic Information and Communication R&D Programme (SCOPE) by Ministry of Internal Affairs and Communications (MIC) of Japan.

## References

- [1] G. Tsoulos (ed.), *MIMO System Technology for Wireless Communications*, Taylor & Francis, 2006.
- [2] H. Bolcskei, D. Gesbert, C.B. Papadias, and A.J. Veen, *Space-Time Wireless Systems*, Cambridge University Press, 2006.
- [3] Y. Karasawa, "MIMO propagation channel modeling," *IEICE Trans. Commun. (Japanese Edition)*, vol.J86-B, no.9, pp.1706–1720, Sept. 2003. (English translation version: *IEICE Trans. Commun.*, vol.E88-B, no.5, pp.1829–1842, May 2005).
- [4] A.T. James, "The distribution of the latent roots of the covariance matrix," *Ann. Math. Statist.*, vol.31, pp.151–158, 1960.
- [5] A. Edelman, "Eigenvalues and condition numbers of random matrix," *SIAM J. Matrix Anal. Appl.*, vol.9, no.4, pp.543–560, 1998.
- [6] T. Taniguchi, S. Sha, and Y. Karasawa, "Statistical distribution of eigenvalues of correlation matrices in i.i.d MIMO channels under Rayleigh fading," *16th Annual IEEE Int. Symp. Personal Indoor and Mobile Radio Commun. (PIMRC'05)*, C02-03, Sept. 2005.
- [7] T. Taniguchi, S. Sha, and Y. Karasawa, "Statistical distribution of eigenvalues in MIMO channels," *The first European Conf. Antennas & Propagation (EuCAP)*, Nice, France, Nov. 2006.
- [8] J. Fu, T. Taniguchi, and Y. Karasawa, "Simplified estimation method for MRC transmission characteristics in Rayleigh i.i.d. MIMO channel," *IEICE Trans. Commun. (Japanese Edition)*, vol.J86-B, no.9, pp.1963–1970, Sept. 2003.
- [9] M. Tsuruta and Y. Karasawa, "Multi-keyhole model for MIMO repeater system evaluation," *IEICE Trans. Commun. (Japanese Edition)*, vol.J89-B, no.9, pp.1746–1754, Sept. 2006.
- [10] D. Chizhic, G.J. Foschini, M.J. Gans, and R.A. Valenzuela, "Keyholes, correlations, and capacities of multielement transmit and receive antennas," *IEEE Trans. Wireless Commun.*, vol.1, no.2, pp.361–368, 2002.
- [11] H. Shin and J.H. Lee, "Effect of keyholes on the symbol error rate of space-time block codes," *IEEE Trans. Commun.*, vol.7, no.1, pp.27–29, 2003.
- [12] M. Tsuruta, T. Taniguchi, and Y. Karasawa, "On statistical distribution of eigenvalues of channel correlation matrix in MIMO multi-keyhole environment," *IEICE Trans. Commun.*, vol.E90-B, no.9, pp.2352–2359, Sept. 2007.
- [13] J.W. Wallas and M.A. Jensen, "Modeling the indoor MIMO wireless channel," *IEEE Trans. Antennas Propag.*, vol.50, no.5, pp.591–599, 2002.
- [14] J.P. Kermaol, L. Schumaacher, F. Fredericksen, and P.E. Mogensen, "Experimental investigation of the joint spatial and polarization diversity for MIMO radio channel," *WPMC'01*, Aalborg, Denmark, Sept. 2001.
- [15] N.K. Das, M. Shinozawa, N. Miyadai, T. Taniguchi, and Y. Karasawa, "Experiments on a MIMO system having dual polarization diversity branches," *IEICE Trans. Commun.*, vol.E89-B no.9, pp.2522–2529, Sept. 2006.
- [16] N.K. Das, T. Inoue, T. Taniguchi, and Y. Karasawa, "An experiment on MIMO system having three orthogonal polarization diversity branches in multipath-rich environment," *IEEE VTC Fall*, pp.1528–1532, LA, Sept. 2004.
- [17] Y. Karasawa and M. Shinozawa, "A compact tri-polarization antenna for MIMO communication systems," *EMTS2007* (to be presented).
- [18] Y. Karasawa, "Statistical multipath propagation modeling for broadband wireless systems," *IEICE Trans. Commun.*, vol.E90-B, no.3, pp.468–484, March 2007.
- [19] Y. Karasawa, N. Gejoh, and T. Izumi, "Modeling and analysis of OFDM transmission characteristics in Rayleigh fading environment in which the delay profile exceeds the guard interval," *IEICE Trans. Commun.*, vol.E88-B, no.7, pp.3020–3027, July 2005.
- [20] X. Nguyen, T. Taniguchi, and Y. Karasawa, "Statistical characteristics of MIMO-OFDM transmission systems in multipath environment where the delay spreading exceeds the guard interval," *IEICE Trans. Commun. (Japanese Edition)*, vol.J87-B, no.9, pp.1467–1476, Sept. 2004. (English translation version: *Electron. Commun. Jpn. 1, Commun.*, vol.88, no.12, 2005).
- [21] Y. Karasawa and M. Shinozawa, "Subband signal processing adaptive array with a data transmission scheme inserting a cyclic prefix," *IEICE Trans. Commun. (Japanese Edition)*, vol.J85-B, no.1, pp.90–96, Jan. 2002. (English translation version: *Electron. Commun. Jpn. 1, Commun.*, vol.86, no.3, pp.1–8, 2003.)
- [22] X.N. Tran, T. Taniguchi, and Y. Karasawa, "Theoretical analysis of subband adaptive array combining cyclic prefix data transmission scheme," *IEICE Trans. Commun.*, vol.E85-B, no.12, pp.2610–2621, Dec. 2002.
- [23] X.N. Tran, T. Taniguchi, and Y. Karasawa, "Subband adaptive array for multirate multicode DS-CDMA systems," *IEICE Trans. Fundamentals*, vol.E86-A, no.7, pp.1611–1618, July 2003.

- [24] N.B. Ramli, N.X. Tran, T. Taniguchi, and Y. Karasawa, "Subband adaptive array for space-time block coding," *IEICE Trans. Fundamentals*, vol.E89-A, no.11, pp.3103–3113, Nov. 2006.
- [25] H.H. Pham, T. Taniguchi, and Y. Karasawa, "The weights determination scheme for MIMO beamforming in frequency-selective fading channels," *IEICE Trans. Commun.*, vol.E87-B, no.8, pp.2243–2249, Aug. 2004.
- [26] T. Taniguchi, H.H. Pham, N.X. Tran, and Y. Karasawa, "Design of MIMO communication systems using tapped delay line structure in receiver side," *IEICE Trans. Fundamentals*, vol.E89-A, no.3, pp.670–677, March 2006.
- [27] H.H. Pham, T. Taniguchi, and Y. Karasawa, "Spatial-temporal adaptive MIMO beamforming for frequency-selective fading channels," *IEICE Trans. Commun.*, vol.E90-B, no.3, pp.578–585, March 2007.
- [28] N.X. Tran, T. Taniguchi, and Y. Karasawa, "Spatio-temporal equalization for space-time block coded transmission over frequency selective fading channel with co-channel interference," *IEICE Trans. Fundamentals*, vol.E88-A, no.3, pp.660–668, March 2005.



**Yoshio Karasawa** received B.E. degree from Yamanashi University in 1973 and M.S. and Dr. Eng. Degrees from Kyoto University in 1977 and 1992, respectively. He joined KDD R&D Labs. in 1977. From July 1993 to July 1997, he was a Department Head of ATR Optical and Radio Communications Res. Labs. and ATR Adaptive Communications Res. Labs. both in Kyoto. Currently, he is a professor in the University of Electro-Communications (UEC), Tokyo, and a core member of Advanced Wireless

Communication research Center (AWCC) in UEC. Since 1977, he has engaged in studies on wave propagation and antennas, particularly on theoretical analysis and measurements for wave-propagation phenomena, such as multipath fading in mobile radio systems, tropospheric and ionospheric scintillation, and rain attenuation. His recent interests are in frontier regions bridging "wave propagation" and "digital transmission characteristics" in wideband mobile radio systems such as MIMO. Dr. Karasawa received the Young Engineer Award from IECE of Japan in 1983 the Meritorious Award on Radio from the Association of Radio Industries and Businesses (ARIB, Japan) in 1998, Research Award from ICF in 2006, and two Paper Awards from IEICE in 2006. He is a senior member of the IEEE and a member of SICE of Japan.